IEEE Access
Multidisciplinary | Rapid Review | Open Access Journal

Received May 20, 2021, accepted June 14, 2021, date of publication June 18, 2021, date of current version July 2, 2021.

Digital Object Identifier 10.1109/ACCESS.2021.3090411

Flexible and Deployable Colon Support Structure for Endoluminal Interventions

MUNEAKI MIYASAKA[1], JIAJUN LIU[1], LIN CAO[1], WENJIE LAI[1], XIAOGUO LI[1], ANTHONY MENG HUAT TIONG[1], CHENG LE GERALD LIM[1], BANJAMIN WEI JIAN QUEK[1], HUANG LENG KAAN[2,3], DMITRII DOLGUNOV[3], KHEK YU HO[4], AND SOO JAY PHEE[1], (Senior Member, IEEE)

[1]School of Mechanical and Aerospace Engineering, Nanyang Technological University, Singapore 639798
[2]Department of Surgery, National University of Singapore, Singapore 119077
[3]Department of Surgery, National University Hospital, Singapore 119074
[4]Department of Medicine, National University of Singapore, Singapore 117597

Corresponding author: Muneaki Miyasaka (mmiyasaka@ntu.edu.sg)

This work was supported by the National Research Foundation (NRF) Singapore under Grant NRFI2016-07.

This work involved human subjects or animals in its research. Approval of all ethical and experimental procedures and protocols was granted by Nanyang Technological University under Approval No. INH2020/012.

ABSTRACT When performing endoluminal surgery inside the colon using a flexible endoscopic robot, there is a problem of losing visualization and task space due to the collapsing of the surrounding wall. This happens mainly because of the intra-abdominal pressure and peristalsis of the colon. Although insufflation is commonly used for expanding the colon, it does not function when a full-thickness incision is created on the colon wall. To support the collapsing colon and ensure sufficient visualization and task space even with a hole, we developed a deployable colon support structure (CSS) that can be seamlessly adapted to the existing procedures. While the CSS is designed to be small and flexible enough to pass through an endoscopic channel that can be tortuous, it becomes sturdy enough to hold the collapsing/squeezing colon after being deployed. Also, the CSS is collapsible after task completion, for retraction through an endoscopic channel. Through the ex-vivo and in-vivo studies with a swine, we have successfully demonstrated the feasibility of supporting the colon wall during endoluminal interventions with the CSS. We confirmed that the CSS was easily deliverable and deployable and the created space was large enough to perform surgical tasks using robotic arms.

INDEX TERMS Surgical instruments, biomedical equipment, medical robotics.

I. INTRODUCTION

The advancement of flexible surgical robot technology has made it possible to access the surgical site through anatomical pathways or natural orifices of the human body and perform endoluminal/intraluminal surgery. Compared to the conventional minimally invasive interventions with rigid instruments, endoluminal surgery can be faster and safer due to spatial flexibility and dexterity. Because endoluminal surgery has such advantages, many flexible surgical robots including both experimental and commercial systems have emerged in recent years [1]–[9]. One problem associated with endoluminal surgery is that surgical operation could be obstructed by the surrounding body lumen. For endoluminal surgery of the colon, ensuring a good visualization can be challenging due to the folds, regional turns between the different parts of the colon, and tissue viscoelasticity. Peristalsis and intra-abdominal pressure (IAP) are other factors that contribute to the occlusion of the endoscope and the loss of vision and task space. Although insufflation could expand the colon wall internally, there are several issues including gas embolism and post-procedure pain due to abdominal distention. If carbon dioxide is used as the insufflation gas, patients with chronic obstructive pulmonary diseases will have a higher risk of carbon dioxide retention [10]. In addition, when perforation is created accidentally or during full-thickness

The associate editor coordinating the review of this manuscript and approving it for publication was Jingang Jiang.

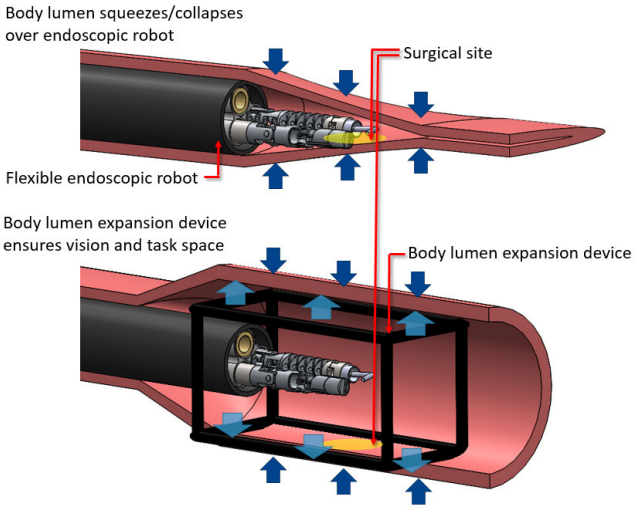

FIGURE 1. Top: Body lumen covers over the endoscope and vision and task space necessary for surgical operation are lost. Bottom: Surgical space is created by introducing a body lumen expansion device.

resection of lesions, the insufflation gas escapes to the peritoneal cavity and the gas is no longer capable of holding the intra-luminal space. Furthermore, the escaped gas could cause cardiopulmonary distress [11]. Therefore, it is advantageous to develop a device that can expand a body lumen to maintain visualization and task space without insufflation during endoluminal procedures (Fig. 1).

Cornhill *et al*. and Milsom *et al*. developed devices that rely on balloons to create a space for endoscopic procedures [12], [13]. Their devices are advantageous due to the functionalities of straightening bends, ironing out the luminal surface folds, and stabilizing the distal tips and working ends of instruments. However, since the devices are to be mounted over an endoscope, the overall diameter increases and the insertion and guiding of the endoscope through the body lumen becomes more challenging. Besides, as those inventions rely on insufflation to expand the sidewall of the body lumen, the body lumen may not be expanded with the existence of a perforation. Milsom *et al*. also developed another body lumen expansion device that is similar to a stent [14]. The device can be detached from an endoscope after deployment and capable of steadying the endoscope and instruments. However, the endoscope dimension becomes large as the device is attached around an endoscope. Piskun *et al*. introduced a multi-lumen-catheter retractor system to improve the visibility and task space for endoscopic procedures [15]. The body lumen is expanded with the retractor elements and an endoscope and an instrument are delivered through the catheter lumens. Since it is an integrated endoscopic system rather than a device to be used with general endoscopes, the cost and the adaptability are potential drawbacks. Reydel *et al*. presented a device directly or indirectly attached to the distal end of an endoscope [16]. The device creates an internal void space with a curved cage constructed by resilient curved bars. The window size of the cage is defined by the curved bars. One issue with the device is that the size of the cage is too small to perform complex tasks. Nakajima *et al*. developed a retractor that comprises a movable wire, multiple stationary wires placed around the movable wire, and an insertion tube connected to the proximal end of the stationary wires [17]. As the movable wire slides toward the insertion tube, the stationary wires sag and expand to create a task space. The major issue with this device is that the deployed structure is not detachable and the space in between the wires is too small for performing endoscopic tasks. We previously developed a device to solve the disadvantages of the above-mentioned devices [18]. However, our previous device faced a problem of tissue squeezing into the created space when tested in-vivo with the porcine colon. Furthermore, ease of deployment of the device was affected by the presence of localised folds in the colon.

In this paper, we present a novel device, the colon support structure (CSS), to internally support the collapsing colon and provide a visualization and task space for endoluminal surgery. The CSS is designed to overcome the issues identified in the existing devices. The key features of the CSS are as follows. (1) small enough to be delivered and retracted through an endoscopic channel so that no specially designed endoscope or modifications on the endoscope are required, (2) flexible enough to go through tortuous pathway inside the colon, (3) easily deployed and collapsed after use to be seamlessly adapted to the existing surgical procedures, (4) rigid enough to support the collapsing colon wall after deployment, (5) detachable from the delivery tools to free up the endoscopic channel, (6) the created space is large enough to perform various surgical tasks, and (7) the created space is sustainable even with a full-thickness incision. The details and the use of the CSS are explained in section II. The performance of the CSS is evaluated ex-vivo and in-vivo with the porcine colon and the results and discussion are presented in sections III and IV. In section V, conclusions regarding the developed CSS are given.

II. MATERIALS AND METHODS

A. MAIN STRUCTURE

The main structure of the CSS consists of PET tubes with 1.9 mm outer diameter and 0.9 mm inner diameter (Nordson Medical, USA). Four joints are created on the tubes by notches with certain angles θ_i ($i = 1, 2, 3, 4$). Each joint is given a specific twist angle ϕ_i with respect to the previous joint such that the structure forms a certain shape after the joints are fully bent (Fig. 2(a)). All the joints are reinforced with a polyester tube with a 0.06 mm wall thickness (Nordson Medical, USA) which is fitted by heat shrinking (Fig. 2(b)). The length of each linkage is labeled as l_i ($i = 1, 2, 3, 4, 5$).

Two symmetrically shaped tubes (Tube 1 and 2) are combined to form the main structure (Fig. 2(c)). The 1st links of each tube are rigidly joined with adhesive and the middle of the 4th links are connected by wrapping a 0.1 mm diameter nitinol wire (Flexmet, Belgium) around so that the links are rotatable about the connection point. Since the nitinol wire

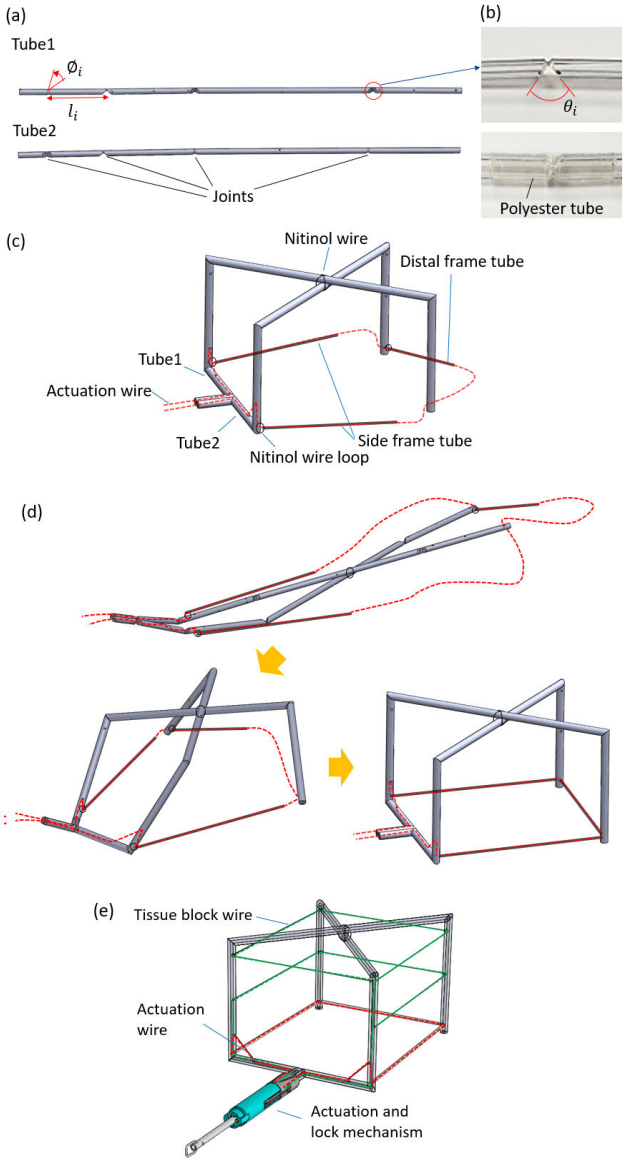

FIGURE 2. (a) PET tube with four joints in straight shape. (b) Zoomed view of a joint which is reinforced with a heat shrink fitted polyester tube. (c) Two symmetrically shaped tubes (Tube 1 and 2) are combined to form the main structure. (d) Deployment flow of the CSS. (e) CSS with the actuation and lock mechanism and tissue block wire.

is elastic, it pushes the tubes to orient them in the proper position and facilitates deployment. To increase the sturdiness of the deployed structure, three 304 stainless steel tubes with an outer diameter of 0.6 mm (MicroGroup, USA) are added as the side and distal frames of the bottom face. The lengths of the side and distal frame tubes are denoted as l_s and l_d respectively. To prevent the bottom frame tubes from falling apart, they are attached to the main structure by nitinol wire loops. A nitinol actuation wire with 0.11 mm diameter (Flexmet, Belgium) is looped through the legs of the main structure while passing through the side and distal frame tubes. By pulling the actuation wire until there is no excess or exposed portion, the joints are forced to rotate up to their limits while the side and distal frame tubes make contact with the

TABLE 1. θ_i and ϕ_i for Tube 1 and Tube 2.

	Parameter $[Unit]$				
	θ_{1-4} $[deg]$	ϕ_1 $[deg]$	ϕ_2 $[deg]$	ϕ_3 $[deg]$	ϕ_4 $[deg]$
Tube 1	90	0	90	140	140
Tube 2	90	180	90	40	40

main structure. Thus, the main structure transforms from the straight to the deployed form (Fig. 2(d)). The actuation wire is managed inside the actuation and lock mechanism which is described in detail in the following section (Fig. 2(e)). Although the CSS is capable of maintaining a large internal space, surrounding tissue could still squeeze in from the open faces. Therefore, another loop of 0.09 mm nitinol wire (Flexmet, Belgium) is embedded to intersect the side faces of the CSS and block tissues. The proximal and bottom faces of the CSS are left open to access an endoscope and perform surgery. Depending on the surgical requirements, the tissue block wire's spacing can be adjusted or the wire can be completely removed if necessary. The tissue block wire also needs to be tensioned for holding tissues pressing in. This is done by terminating the tissue block wire at the actuation rod and pulling it together with the actuation wire.

As the size of the colon varies depending on the locations and individuals, the size of the CSS needs to be selected carefully before each use. The diameter of the adult's colon ranges from 30 to 90 mm [19], [20]. While the cecum has the largest diameter of 90 mm and the anal canal has the smallest diameter of 30 mm, the rest of the colon (ascending, transverse, and descending colon) are usually less than 60 mm and the sigmoid colon is slightly smaller in diameter. Besides, to determine the proper CSS's dimension, we need to take into account the size of the robotic arms to perform surgical tasks. In this work, we refer to the flexible endoscopic robot developed in Nanyang Technological University [21]. The articulated arms are 24 mm long and the robot requires about 40 mm of space or depth when tightening a knot after suturing. The values of θ_i and ϕ_i for the CSS we manufactured for the experiments are summarized in Table. 1. We prepared three different structure sizes and l_i and the lengths of the side and distal tubes are shown in Table. 2 (both Tube 1 and 2 have the same l_i.). The lengths of links 2 and 3 are determined such that the proximal face of the deployed structure is slightly larger than the size of the colon to push the inner wall outward and anchor the CSS. Also, the length of link 5 is made short to have small distal face to help prevent catching tissue and getting stuck during the deployment process.

The volume of the deployed CSS can be estimated from the lengths of the linkages. We assume all the joints reach their maximum limits as indicated in Table. 2 and the linkages 2 and 5 are perpendicular to the bottom face. The cross-section of the deployed CSS is a rectangular shape from the proximal to the distal face. Then, the volume (V) is represented by integrating the cross-sectional area along the direction of x indicated in Fig. 3:

$$V = \int_0^L L_x(x) L_y(x) dx \tag{1}$$

TABLE 2. Linkage dimensions and suitable colon sizes for three different size CSS.

	l_1 $[mm]$	l_2 $[mm]$	l_3 $[mm]$	l_4 $[mm]$	l_5 $[mm]$	l_s $[mm]$	l_d $[mm]$	Colon Φ $[mm]$
Small	7	30	20	50	15	50	10	50
Medium	7	35	25	55	15	54	10	60
Large	7	40	30	60	15	58	10	70

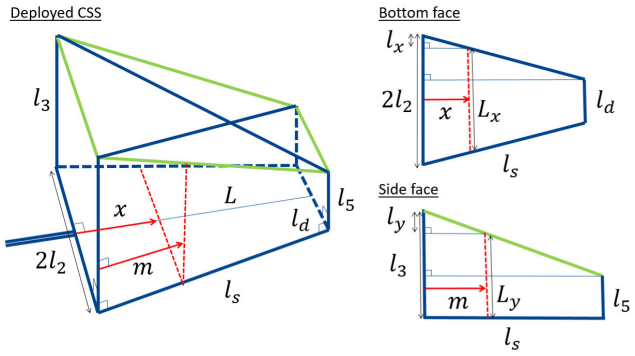

FIGURE 3. Dimensions of the deployed CSS. The main structure (PET tubes and side and distal frame tubes) is indicated in the blue line and the nitinol wire (tissue block wire) is indicated in the green line.

where

$$L = \sqrt{l_s^2 - (l_2 - \frac{l_d}{2})^2} \tag{2}$$

$$L_x = 2(l_2 - l_x) \tag{3}$$

$$L_y = l_3 - l_y \tag{4}$$

$$l_x = \frac{l_2 - \frac{l_d}{2}}{L} x \tag{5}$$

$$l_y = \frac{l_3 - l_5}{l_s} m \tag{6}$$

$$m = \frac{l_s}{L} x \tag{7}$$

and the result of the integration yields

$$V = \frac{L}{6}(4l_2l_3 + 2l_2l_5 + l_3l_d + 2l_5l_d) \tag{8}$$

B. ACTUATION AND LOCK MECHANISM

To transform the structure from the straight to the fully deployed form, the actuation and tissue block wires will need to be pulled for about 130 - 150 mm depending on the size of the CSS. If the wires are pulled linearly, the CSS will become too long considering a mechanism to hold the pulled wire. To keep the CSS's length as short as possible, a threaded rod is employed and the wires are wound around the threads. Also, after the structure is fully deployed, the threaded rod is locked to avoid unwinding and releasing the tension in the wires. Hence, we developed the actuation and lock mechanism shown in Fig. 4(a). It consists of three components; the actuation base, actuation rod, and lock cap. The actuation base is attached to the main structure by adhesive. The actuation base has a threaded hole in the middle for the actuation rod to fit. The wire guide grooves next to the lock cap guide ridges are to guide the wires from the main structure to the actuation rod. The actuation rod has an M3 size threaded rod on one end and a lock key right next to it. The wires are terminated at the lock key such that the wires are wound around the threaded rod as it is unscrewed (Fig. 4 (b)). To fully deploy, the actuation rod needs to be rotated roughly 14 - 16 revolutions. After the actuation rod is rotated, it needs to be fixed to avoid the wires from unwinding. The lock cap consists of a guide slot, stop slot, delivery tube lock, and key slots. As the cap slides in along the lock cap guide ridges of the actuation base, the lock key on the actuation rod fits into one of the key slots and is thus prevented from rotating.

All the manipulations of the CSS are provided distally by the actuation rod and delivery tube (Fig. 4 (c)). The actuation rod has an L-hook at the tip which is fitted to the L-hook hole on the actuation rod. Thus, the distal rotation of the actuation rod is transmitted to the actuation rod for deployment. The tip of the delivery tube has an L shape socket and it is fitted to the delivery tube lock. This mechanism makes the delivery tube easily and securely attachable/detachable to the CSS. By connecting the delivery tube and the CSS, the CSS's position and orientation can be adjusted from the distal end of the delivery tube. Therefore, the CSS can be delivered or retracted simply by pushing or pulling the delivery tube through an endoscopic channel.

The actuation base and the lock cap are 3d printed with L316 stainless steel (Protolabs, USA). The entire actuation rod and the cap guide slot are made out of a stainless steel tube (MicroGroup, USA) and a threaded rod (Misumi, Japan). With the actuation and lock mechanism, the total straight length of the CSS becomes about 150 mm (125 mm main structure and 25 mm actuation and lock mechanism). The largest part of the CSS has a diameter of 4.5 mm.

C. FLOW OF USAGE

1) Delivery: The actuation rod and delivery tube are first connected to the CSS. Then, the CSS is inserted into an endoscopic channel until the structure reaches the distal end of the endoscope (Fig. 5(a)). Insufflation is turned on to expand the colon and the endoscope is placed at a position deeper than the surgical site. While holding the L-hook rod and delivery tube, the endoscope is retracted until the entire CSS is exposed.
2) Deployment: The actuation rod is rotated to unscrew the actuation rod and wind the actuation wire while holding the delivery tube to avoid the CSS from rotating together. In this process, there must be sufficient insufflation to prevent surrounding tissue from applying external loads onto the CSS so as to not hinder the deployment of the CSS. After the CSS reaches its deployed form, the lock is activated by pushing the

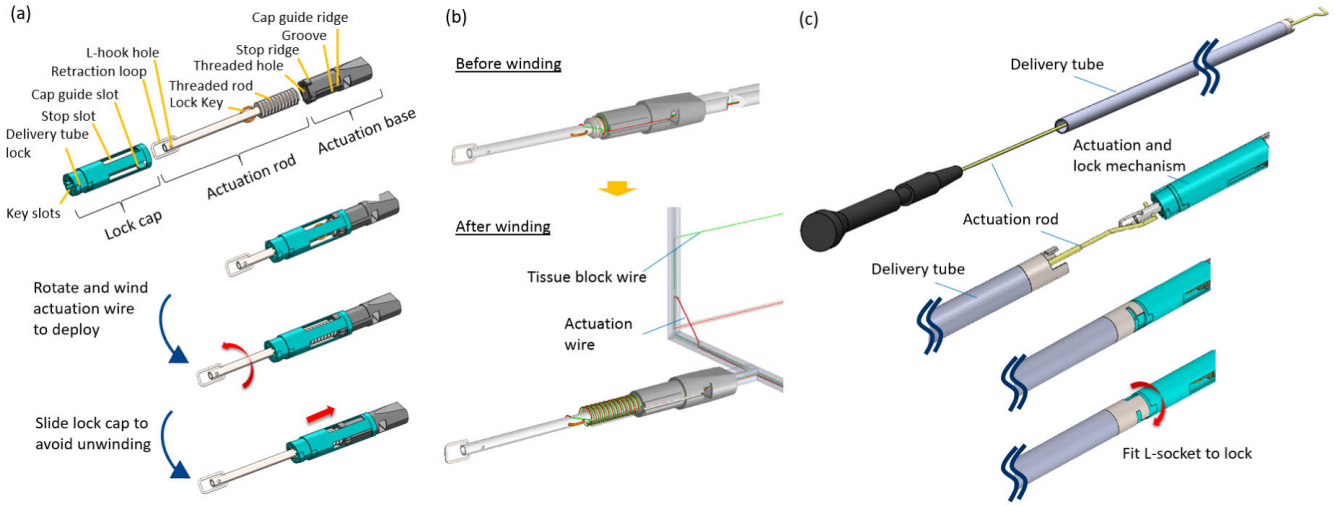

FIGURE 4. (a) Details of the actuation and lock mechanism. (b) Winding the actuation wire and tissue block wire. (c) CSS is connected to the actuation rod and delivery tube for distal manipulation.

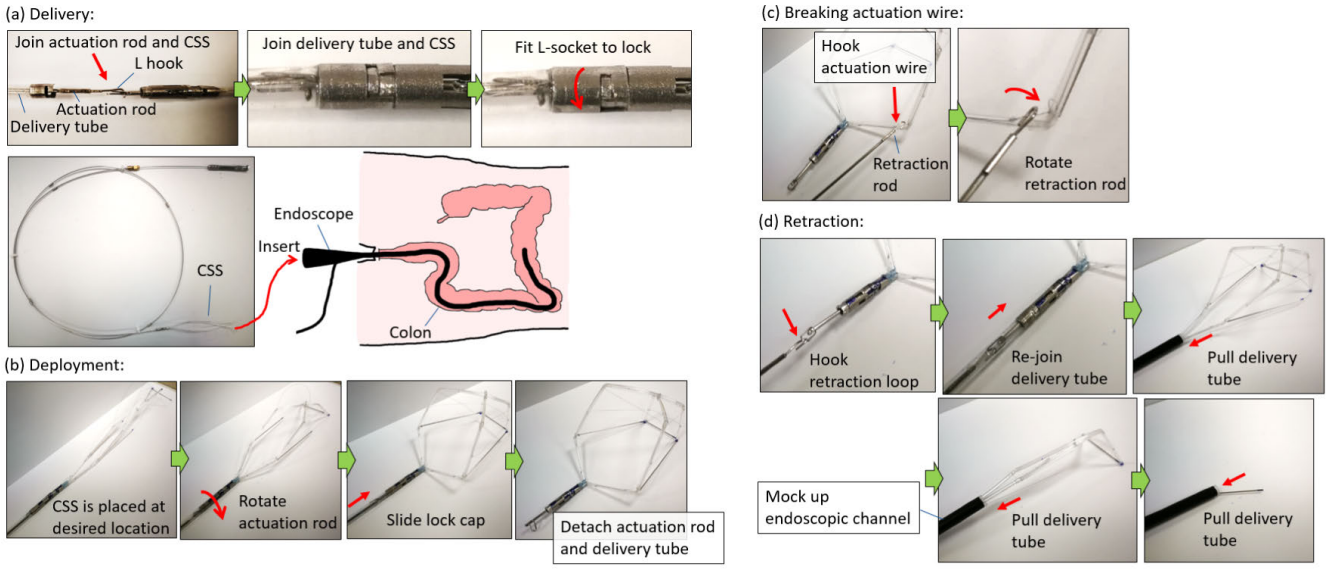

FIGURE 5. Usage flow the CSS. The processes of (a) delivery, (b) deployment, (c) breaking actuation wire, and (d) retraction are shown.

delivery tube and sliding the lock cap. This prevents the screw from rotating and the actuation wire from unwinding. Then, the delivery tube and actuation rod are detached from the CSS (Fig. 5(b)). The insufflation can now be stopped and surgery can be performed inside the CSS.

3) Breaking actuation wire: To prepare for CSS retraction, it first needs to be collapsed, by releasing the tension in the main actuation wire. To do that, the retraction rod with U-hook at the tip is introduced to hook one of the exposed actuation wires in the proximal face of the CSS (between link 2 and 3). Then, the wire tension is increased by rotating the hook and twisting the actuation wire until it is broken (Fig. 5(c) and Fig. 6(a)).
4) Retraction: After the wire tension is released, the retraction loop is hooked onto the retraction rod and the delivery tube is re-joined. Then, the CSS can be retracted through an endoscopic channel by simply pulling the delivery tube (Fig. 5(d) and Fig. 6(b)).

III. RESULTS

A. EX-VIVO EXPERIMENTS

All the experiments performed in this section investigates the general use of the CSS and not replicating any particular surgical procedure. Although the size of the CSS used in the experiments is determined based on the surgical robot developed in Nanyang Technological University, any surgical procedure can be performed under the CSS as long as the size of the CSS is adequate for the specific procedure.

1) STRUCTURAL STRENGTH

The structural strength of the CSS is experimentally investigated. The CSS was placed inside a double-layered plastic bag and the air is supplied in between the inner and outer bags

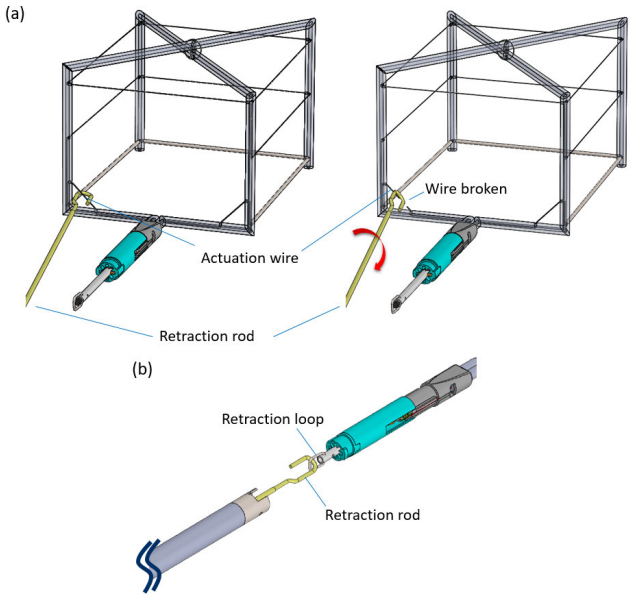

FIGURE 6. **(a)Breaking the actuation wire with the retraction rod. (b)Catching the retraction loop with the retraction rod to re-joining the CSS.**

(Fig. 7). An inner tube was placed inside the CSS such that excess air can escape and the inner bag can directly compress the CSS. Firstly, a medical insufflation unit (UHI-4, Olympus, Japan) was used to apply an external pressure of 3.33 kPa (25 mmHg) which is the highest pressure the insufflator can provide. Next, to apply even higher pressures, a manual pump was used. We applied two and three times higher pressures of the insufflator's limit (6 and 10 kPa respectively). For all the external pressures we applied, no noticeable deformation of the CSS was observed.

2) VALIDATION OF INTERNAL SPACE

The colon tissue is viscoelastic and tends to deform and fill in an open space. Therefore, we need to investigate whether the CSS can maintain sufficient internal space. The CSS was deployed inside the porcine colon with roughly 60 mm diameter. With no insufflation, the colon tissue covered over the CSS due to gravity. Since almost no tissue entered the space, a large surgical space was maintained (Fig. 8(a)). To simulate a realistic live colon environment, the colon was enclosed by a plastic bag and external pressure was applied using the UHI-4 Olympus insufflator with the highest appliable pressure of 3.33 kPa. We applied two different external pressures of 1.67 and 3.33 kPa. Since the insufflator's highest pressure is 3.33 kPa, it should be a large enough pressure to simulate the worst squeezing effect of the colon. For 1.67 kPa, a small amount of tissue squeezed in but a decent space for surgery remained (Fig. 8(b)). When 3.33 kPa was applied, although the internal space was invaded by the tissue more significantly, sufficient visualization of the bottom surface where surgery will take place is maintained. (Fig. 8(c)). For all cases, no deformation of the structure was observed and therefore the structural rigidity was confirmed to be sufficient.

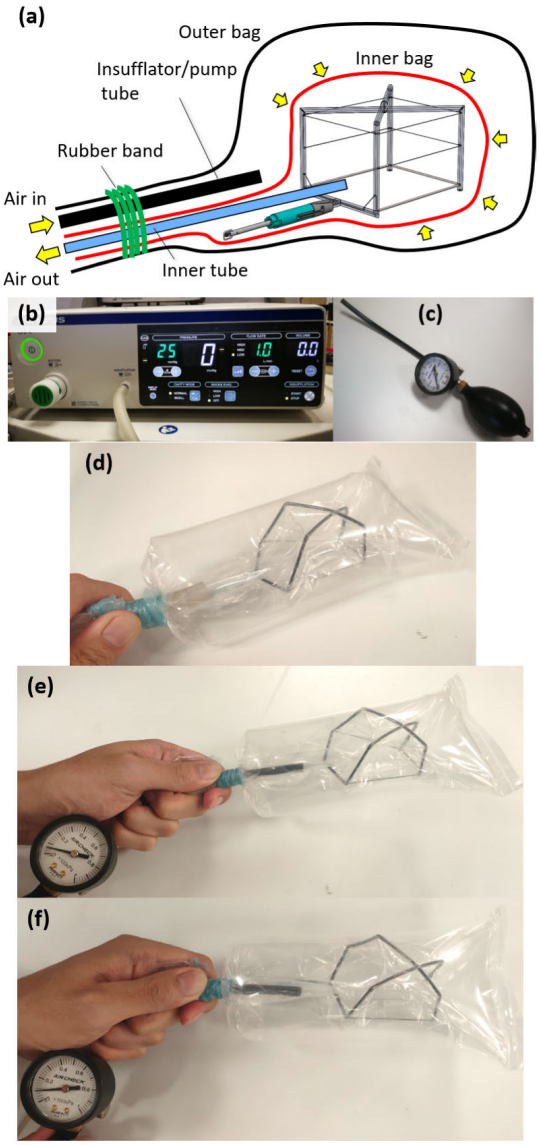

FIGURE 7. **(a) Experimental setup to test the structural strength of the CSS. External pressure was applied using (b) Olympus UHI-4 insufflator and (c) manual pump. (d)3.33 kPa (25 mmHg), (e)6 kPa, and (f)10 kPa of external pressures were applied.**

3) DEPLOYABILITY TEST

The live human colon has folds and bends and they could be obstacles when deploying the CSS. To investigate the deployability over the folds, rubber bands were placed over the porcine colon and the folds were artificially created as the folds do not appear in the dead colon. Because the rubber bands are stiffer and not as visco-elastic as the real folds, deployment over the artificial folds is more challenging. It is very difficult to find a material that is similar to the human colon folds. Even the off-the-shelf colonic models are stiffer than the actual folds [22]. Therefore, the objective of this experiment is to demonstrate the CSS can be deployed even under extremely challenging situations. In the first trial, the CSS was placed over the three folds. As the actuation wire was wound, the distal tube caught the fold and

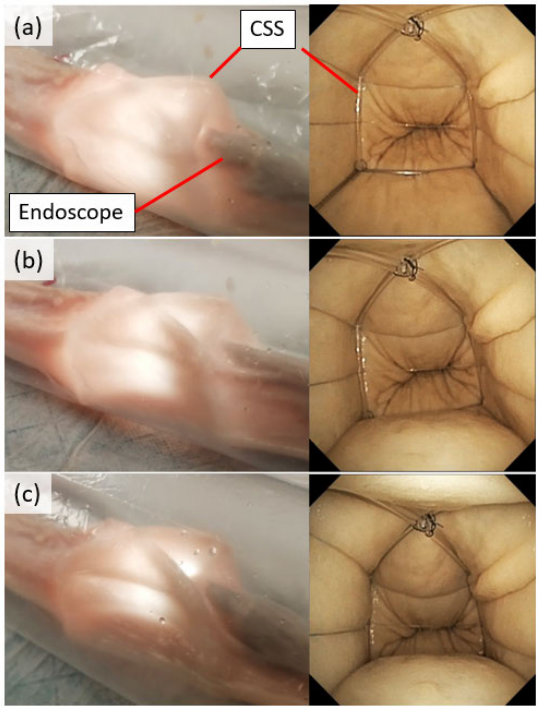

FIGURE 8. Ex-vivo study with the porcine colon. External and internal views of the CSS under (a) no external pressure, (b) 1.67 kPa, and (c) 3.33 kPa (the highest appliable pressure of the insufflator).

the deployment was interrupted. When higher tension was applied, the actuation wire broke before the CSS was fully deployed (Fig. 9(a-c)). In the second trial, the CSS was placed so that the tip was away from a fold. This time, the CSS was deployed successfully without being stuck or catching on to tissue (Fig. 9(d-f)).

Next, the CSS was delivered inside a curved colon with a bend radius of roughly 10 cm and 25 cm (Fig. 9(g,j)). Those numbers were selected by assuming the typical anatomy of the rectum and the sigmoid colon which are about 15 cm and 45 cm long respectively with roughly 90° bend [23], [24]. Although the CSS was bent before deployment, there was no issue with the deployment process for both bend radii (Fig. 9(h,i,k,l)).

B. IN-VIVO EXPERIMENTS

The CSS was tested inside the live swine (about 60 kg) under general anesthesia (Fig. 11(a,b)) with the approval from the Institutional Animal Care and Use Committee (INH2018/017), Singapore. The CSS used for the in-vivo experiment is shown in Fig. 10. We firstly introduced a CSS without the lock mechanism to check the inner diameter of the targeted location of the colon. After confirming the colon size, a proper size CSS was selected and introduced from an endoscopic channel under insufflation. The CSS was deployed smoothly and detached successfully (Fig. 11(c)). The delivery tube and actuation rod were then removed (Fig. 11(d)). An injector was introduced to dye and lift the targeted tissue and a submucosal dissection was created with an electrical cautery knife (Fig. 11(e,f)). After stopping the

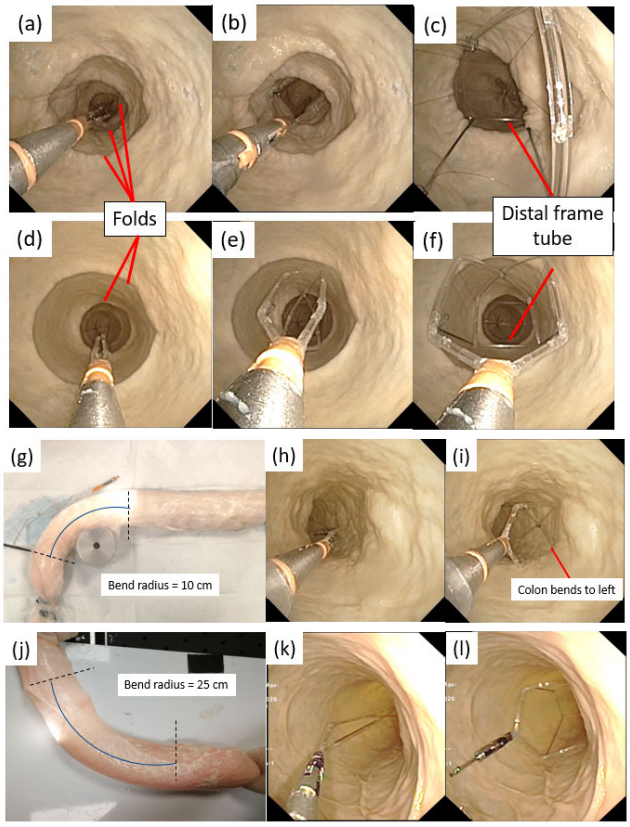

FIGURE 9. Ex-vivo deployment test inside the porcine colon. (a-c) The deployment fails when the distal frame tube is right behind the fold. (d-f) Successfully deployed when the distal frame tube is placed in front of the fold. (g,j) The CSS is deployed inside the colon with 10 cm and 25 cm bend radii. (h,i) Endoscopic view before and after deployment for 10 cm bend radius. (k,l) Endoscopic view before and after deployment for 25 cm bend radius.

insufflation, we observed about half of the CSS's inner space was occupied by the tissue rising from the bottom face. The robotic arms were inserted to suture the incision (Fig. 11(g)). Although there was a space left inside the CSS, insufflation was applied occasionally to facilitate the suturing task. After the suturing task was completed, the robotic arms were retracted and the U hook was inserted to catch and break the exposed actuation wire (Fig. 11(h)). The retraction loop was caught with the U-hook and the CSS was re-joined with the delivery tube (Fig. 11(i,j)). Then, the CSS was retracted from the endoscopic channel without any issues (Fig. 11(k)). Next, the CSS was tested under a full-thickness incision (Fig. 11(l)). We again observed the tissue squeezed into the inner space of the CSS and the external organ was observed through the incision (Fig. 11(m)). Therefore, insufflation was applied occasionally to keep the optimal visibility and task space (Fig. 11(n)). After the closure of the incision with the robotic arms, the CSS was retracted successfully.

IV. DISCUSSION

Although the deployability of the CSS was verified both ex-vivo and in-vivo setups, different combinations of colon diameter and CSS size would cause the failure of deployment (i.e. deploying large CSS inside a small colon). In the in-vivo

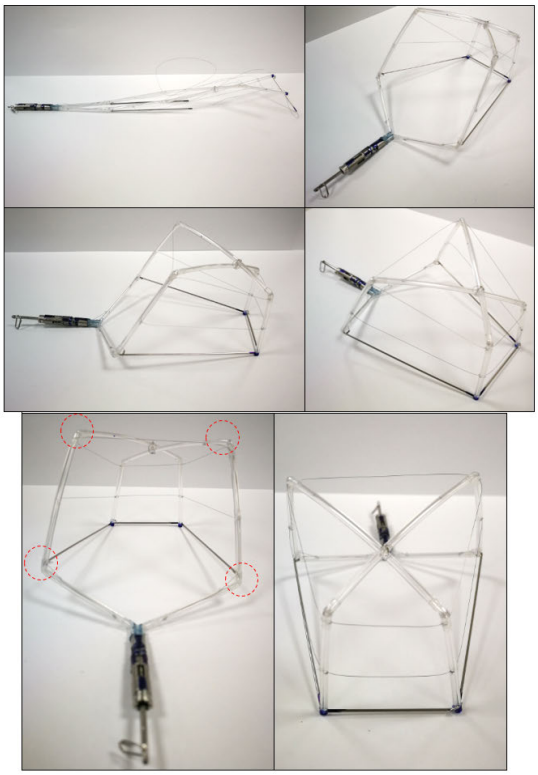

FIGURE 10. The CSS used for the in-vivo porcine study. The red circles indicate the sharp edges that caused the tissue damage observed in Fig. 11 (d).

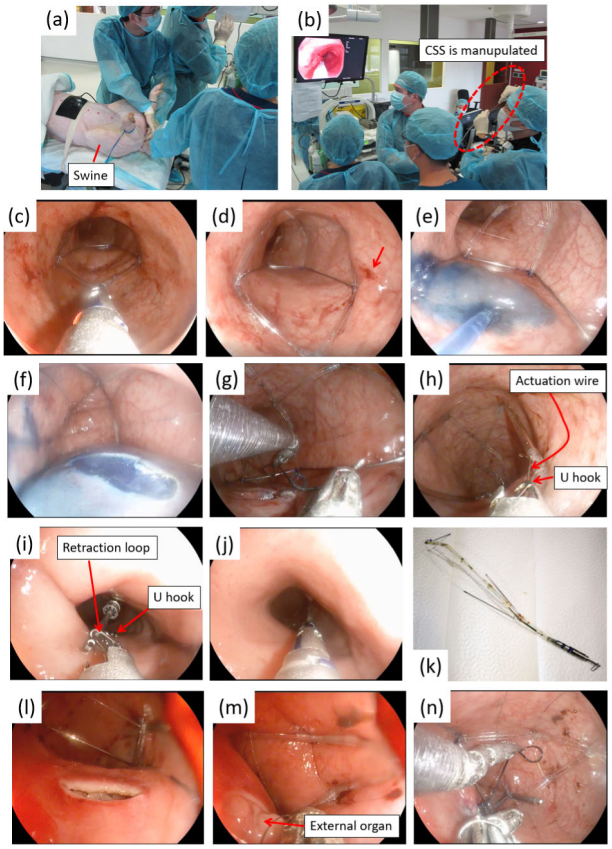

FIGURE 11. In-vivo porcine study. (a) Swine under general anesthesia. (b) The CSS is manipulated outside of the porcine colon. (c) The CSS is being deployed inside the porcine colon. (d) Deployed and detached CSS. The arrow indicates the tissue damage caused by the sharp edge of the CSS. (e) Blue dye is injected to lift the submucosa. (f) A submucosal incision is created. (g) Suturing is performed with robotic arms under the CSS. (h) Breaking the actuation wire. (i) Catching the CSS with U-hook. (j) CSS is re-joined with the delivery tube. (k) Retracted CSS. (l) Full-thickness incision is created. (m) Colon tissue squeezes in without insufflation. (n) Full-thickness suturing is performed with robotic arms.

experiment, we used a CSS without the lock mechanism but it would be ideal if the colon size is measured more accurately and easily to select a proper-sized CSS prior to delivery. The worst-case scenario for deployment would be the combination of the folds and sharp bends that could happen in the live colon. In this case, the tip of the CSS needs to be positioned away from those folds and bends and the CSS needs to be re-position after deployment.

Because not all the endoluminal robots have a large enough channel to deliver the CSS, it would be more convenient if the CSS is deliverable through a channel of a commonly used endoscope. Usually, a colonoscope for diagnosis has a 3.2 mm channel with a 45° bend near the entrance. Therefore, the application can be expanded by modifying the CSS to pass through such a channel. In this work, we only have shown the usability of the CSS for the colon. However, it can be applied to the other body lumens by changing the design parameters.

For the ex-vivo experiment, no insufflation was required to maintain the inner space of the CSS even under the highest external pressure from the insufflator. However, for the in-vivo experiment, the colon wall entered from the bottom face (the face to perform surgery) of the CSS and blocked about half of the inner space. This happened because the dead colon tissue was less visco-elastic compared to the live colon tissue. The insufflation needs to be applied continuously without the CSS but with the CSS, we roughly applied 5 seconds of insufflation every 25 seconds. Therefore, the amount of gas utilised was reduced to 1/6. In order to avoid the tissue from entering the CSS's inner space without insufflation, the tissue block wire should be added and the open space of the bottom face needs to be controlled properly.

In the in-vivo trial, the sharp edge of the front face of the CSS (as shown in Fig. 10) created shallow scratches and caused minor bleeding on the colon wall (Fig. 11(d)). In the future, we will modify the joint design and blunt the sharp edge for safety. It can be done by increasing the number of notches for each joint. Currently, each joint has one 90 degree notch. It can be divided into 6 15-degree notches for instance, to have less sharp edges with more contact area. This will only affect the shape of the proximal face will not change the deployability of the CSS.

Although it was possible, in the retraction process, catching the exposed actuation wire to break and hooking the retraction loop was time-consuming. By exposing a longer portion of the actuation wire, the time to catch it with a hook can be reduced. Besides, attaching a magnet at the proximal end of the CSS and using magnetic attraction could simplify the re-joining and retraction process.

V. CONCLUSION

We have developed a colon support structure (CSS) to overcome a crucial problem of endoluminal surgery which is the occlusion of the vision and task space by the surrounding wall. The CSS was designed to be small and flexible to be delivered through an endoscopic channel, easily deploy and yet collapsible on demand, and capable of supporting the collapsing colon wall even with a full-thickness incision. Although slight modifications will be required for the optimal outcome, through the ex-vivo and in-vivo porcine studies, we have shown the feasibility of ensuring the vision and task space for endoluminal interventions of the colon using the CSS. The next milestone will be to validate the CSS with human in-vivo trials.

ACKNOWLEDGMENT

The authors would like to thank the members of the Robotics Research Centre at Nanyang Technological University for their support and contribution throughout the entire project.

REFERENCES

[1] S. J. Phee, N. Reddy, P. W. Y. Chiu, P. Rebala, G. V. Rao, Z. Wang, Z. Sun, J. Y. Y. Wong, and K. Ho, "Robot-assisted endoscopic submucosal dissection is effective in treating patients with early-stage gastric neoplasia," *Clin. Gastroenterol. Hepatol.*, vol. 10, no. 10, pp. 1117–1121, Oct. 2012.

[2] N. Patel, A. Darzi, and J. Teare, "The endoscopy evolution: 'The superscope era,'" *Frontline Gastroenterol.*, vol. 6, no. 2, pp. 101–107, Apr. 2015.

[3] C. A. Seneci, J. Shang, K. Leibrandt, V. Vitiello, N. Patel, A. Darzi, J. Teare, and G.-Z. Yang, "Design and evaluation of a novel flexible robot for transluminal and endoluminal surgery," in *Proc. IEEE/RSJ Int. Conf. Intell. Robots Syst.*, Sep. 2014, pp. 1314–1321.

[4] M. Mandapathil, U. Duvvuri, C. Güldner, A. Teymoortash, G. Lawson, and J. A. Werner, "Transoral surgery for oropharyngeal tumors using the medrobotics flex system—A case report," *Int. J. Surg. Case Rep.*, vol. 10, pp. 173–175, Jan. 2015.

[5] D. J. Abbott, C. Becke, R. I. Rothstein, and W. J. Peine, "Design of an endoluminal NOTES robotic system," in *Proc. IEEE/RSJ Int. Conf. Intell. Robots Syst.*, Oct. 2007, pp. 410–416.

[6] B. Bardou, F. Nageotte, P. Zanne, and M. de Mathelin, "Design of a robotized flexible endoscope for natural orifice transluminal endoscopic surgery," in *Computational Surgery and Dual Training*. Boston, MA, USA: Springer, 2010, pp. 155–170.

[7] M. Hwang and D.-S. Kwon, "K-flex: A flexible robotic platform for scar-free endoscopic surgery," *Int. J. Med. Robot. Comput. Assist. Surg.*, vol. 16, no. 2, p. e2078, Apr. 2020.

[8] K. C. Lau, E. Y. Y. Leung, P. W. Y. Chiu, Y. Yam, J. Y. W. Lau, and C. C. Y. Poon, "A flexible surgical robotic system for removal of early-stage gastrointestinal cancers by endoscopic submucosal dissection," *IEEE Trans. Ind. Informat.*, vol. 12, no. 6, pp. 2365–2374, Dec. 2016.

[9] O. M. Omisore, S. Han, L. Ren, Z. Zhao, Y. Al-Handarish, T. Igbe, and L. Wang, "A teleoperated snake-like robot for minimally invasive radiosurgery of gastrointestinal tumors," in *Proc. IEEE Int. Conf. Auto. Robot Syst. Competitions (ICARSC)*, Apr. 2018, pp. 123–129.

[10] T. Menes and H. Spivak, "Laparoscopy: Searching for the proper insufflation gas," *Surgical Endoscopy*, vol. 14, no. 11, pp. 1050–1056, 2000.

[11] S. K. Lo, L. L. Fujii-Lau, B. K. Enestvedt, J. H. Hwang, V. Konda, M. A. Manfredi, J. T. Maple, F. M. Murad, R. Pannala, K. L. Woods, and S. Banerjee, "The use of carbon dioxide in gastrointestinal endoscopy," *Gastrointestinal Endoscopy*, vol. 83, no. 5, pp. 857–865, May 2016.

[12] J. F. Cornhill, J. Milsom, S. Sharma, T. A. Nguyen, C. Dillon, G. Greeley, R. Sathe, M. DeNardo, A. Whitney, J. Van Hill, and A. Z. Assal, "Method and apparatus for manipulating the side wall of a body lumen or body cavity so as to provide increased visualization of the same and/or increased access to the same, and/or for stabilizing instruments relative to the same," U.S. Patent 9 986 893, Jun. 5, 2018.

[13] J. Milsom, H. Riina, J. F. Cornhill, E. Dickinson, C. Strohl, J. Mahoney, and P. Coppola, "Method and apparatus for stabilizing, straightening, expanding and/or flattening the side wall of a body lumen and/or body cavity so as to provide increased visualization of the same and/or increased access to the same, and/or for stabilizing instruments relative to the same," U.S. Patent 8 979 884, Mar. 17, 2015.

[14] J. Milsom, H. Riina, J. F. Cornhill, R. Andrews, and E. Dickinson, "Method and apparatus for straightening and flattening the side wall of a body lumen or body cavity so as to provide three dimensional exposure of a lesion or abnormality within the body lumen or body cavity, and/or for stabilizing an instrument relative to the same," U.S. Patent 9 649 100, May 16, 2017.

[15] G. Piskun, J. To, M. Fabro, B. Tang, and S. Kantsevoy, "Floating, multi-lumen-catheter retractor system for a minimally-invasive, operative gastrointestinal treatment," U.S. Patent 8 932 211, Jan. 13, 2015.

[16] B. Reydel and S. Kantsevoy, "Endoscopic assistance devices and methods of use," U.S. Patent 15 897 320, Aug. 16, 2018.

[17] K. Nakajima and H. Yamashita, "Retractor," U.S. Patent 10 080 556, Sep. 25, 2018.

[18] M. Miyasaka, J. Liu, L. Cao, and S. J. Phee, "Pneumatically actuated deployable tissue distension device for notes for colon," in *Proc. Int. Conf. Robot. Autom. (ICRA)*, 2019, pp. 9828–9833.

[19] K. M. Horton, F. M. Corl, and E. K. Fishman, "CT evaluation of the colon: Inflammatory disease," *RadioGraphics*, vol. 20, no. 2, pp. 399–418, Mar. 2000.

[20] T. Jaffe and W. M. Thompson, "Large-bowel obstruction in the adult: Classic radiographic and CT findings, etiology, and mimics," *Radiology*, vol. 275, no. 3, pp. 651–663, Jun. 2015.

[21] L. Cao, X. Li, P. T. Phan, A. M. H. Tiong, H. L. Kaan, J. Liu, W. Lai, Y. Huang, H. M. Le, M. Miyasaka, K. Y. Ho, P. W. Y. Chiu, and S. J. Phee, "Sewing up the wounds: A robotic suturing system for flexible endoscopy," *IEEE Robot. Autom. Mag.*, vol. 27, no. 3, pp. 45–54, Sep. 2020.

[22] M. Pioche, M. Matsumoto, H. Takamaru, T. Sakamoto, T. Nakajima, T. Matsuda, S. Abe, Y. Kakugawa, Y. Otake, and Y. Saito, "Endocuff-assisted colonoscopy increases polyp detection rate: A simulated randomized study involving an anatomic colorectal model and 32 international endoscopists," *Surgical Endoscopy*, vol. 30, no. 1, pp. 288–295, Jan. 2016.

[23] Y. Nigam, J. Knight, and N. Williams, "Gastrointestinal tract 5: The anatomy and functions of the large intestine," *Nursing Times*, vol. 115, no. 10, pp. 50–53, 2019.

[24] M. Phillips, A. Patel, P. Meredith, O. Will, and C. Brassett, "Segmental colonic length and mobility," *Ann. Roy. College Surgeons England*, vol. 97, no. 6, pp. 439–444, Sep. 2015.

MUNEAKI MIYASAKA received the Ph.D. degree in mechanical engineering from the University of Washington, USA, in 2017. He is currently a Research Fellow with Nanyang Technological University, Singapore. His research interests include medical robots and systems and tendon/wire driven mechanisms.

JIAJUN LIU received the B.Eng. degree (Hons.) from Nanyang Technological University (NTU), Singapore, in 2014, where he is currently pursuing the Ph.D. degree in mechanical and aerospace engineering. He is a Research Assistant with the Robotics Research Center, MAE, NTU. His research interests include modeling of continuum robots, soft robotics, and surgical robotics.

LIN CAO received the Ph.D. degree in mechanical engineering from the University of Saskatchewan, Canada, in 2015. He was a Visiting Scholar with the Department of Precision and Microsystems Engineering, Delft University of Technology, The Netherlands, in 2013. He is currently a Research Fellow with the Robotics Research Center, Nanyang Technological University, Singapore. His research interests include surgical robots, soft robots, and compliant systems.

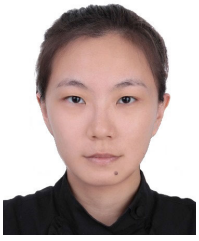

WENJIE LAI received the B.Eng. degree (Hons.) from Nanyang Technological University (NTU), Singapore, in 2015, under an SM3 Scholarship, where she is currently pursuing the Ph.D. degree. She is a Research Assistant with the Robotics Research Center, MAE, NTU. Her research interests include fiber optics sensors, force feedback, haptic display, pose tracking, robotic surgical systems, and soft robotics.

XIAOGUO LI received the B.Eng. degree (Hons.) in mechatronics from Nanyang Technological University (NTU), Singapore, in 2015, under an SM2 Scholarship, where he is currently pursuing the Ph.D. degree. He is working as a Senior Data Scientist with the E-commerce industry. He has developed research interests in both mechanical engineering and data science and specializes in adopting deep learning techniques in solving challenges faced by robotic systems.

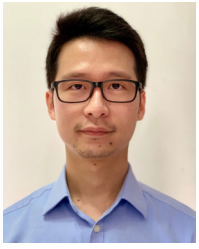

ANTHONY MENG HUAT TIONG received the M.Eng. degree in aeronautical engineering from Imperial College London, in 2015. He is currently pursuing the Ph.D. degree with Nanyang Technological University, Singapore. His research interests include long-tailed classification and semi-supervised learning in computer vision domain.

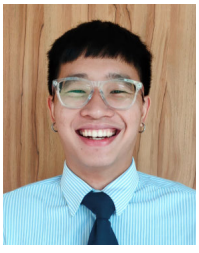

CHENG LE GERALD LIM received the B.E. degree in engineering product development from the Singapore University of Technology and Design, in 2020, with a focus on healthcare engineering. He is currently a Project Officer with Nanyang Technological University, Singapore. His research interests include surgical/medical robots, low-cost, low-tech medical interventions for developing nations, and medical sensors.

BANJAMIN WEI JIAN QUEK received the B.S. degree in mechanical engineering from the National University of Singapore, Singapore, in 2018. He is currently a Project Officer with Nanyang Technological University, Singapore. His research interests include surgical/medical robots and systems.

HUANG LENG KAAN received the M.B.B.S. degree, in 2012, and the Master of Medicine (Surgery) degree from the National University of Singapore, in 2014, where she is currently pursuing the Ph.D. degree in medicine. In 2013, she became a member of The Royal College of Surgeons of Edinburgh, where she became a fellow, in 2018. She is a General Surgery Associate Consultant with the Ng Teng Fong General Hospital, Singapore. Her research interests include surgical robotics and medical device technologies.

DMITRII DOLGUNOV held clinical fellowship at UGI Surgery, NUHS Singapore from 2013 to 2014. He is currently a certified general surgeon/an oncologist/an endoscopist in Russia. He is a Resident Physician II with the Colorectal Surgery Department, NUHS. He is specialized in complex colonoscopic procedures with interest in colonic endoscopic submucosal dissection (ESD).

KHEK YU HO received the M.B.B.S. degree from the University of Sydney and the M.D. degree from the National University of Singapore. After completing his fellowship in gastroenterology with the National University Hospital, Singapore, he undertook training in therapeutic gastrointestinal endoscopy and endoscopic ultrasound at the Brigham and Women's Hospital, and Hospital of the University of Pennsylvania, respectively. He is currently a Professor of Medicine with the National University of Singapore. His research interests include innovative endoscopic technology in the diagnosis and management of GI cancer, epidemiology, and management of Barrett's esophagus and its related neoplasia.

SOO JAY PHEE (Senior Member, IEEE) received the Ph.D. degree from Scuola Superiore Sant'Anna, Pisa, Italy, under a European Union Scholarship. He is currently a Full Professor and the Dean of the College of Engineering, Nanyang Technological University, Singapore. He is the Tan Chin Tuan Centennial Professor. His research interests include medical robotics and mechatronics in medicine.